Proceedings of the 4th WSEAS International Conference on Fluid Mechanics and Aerodynamics, Elounda, Greece, August 21-23, 2006 (pp289-294)

Numerical Study on Impeller-Diffuser Interactions with Radial Gap Variation

JIANJUN FENG, FRIEDRICH-KARL BENRA, HANS JOSEF DOHMEN
Chair of Turbomachinery
Department of Mechanical Engineering
University of Duisburg-Essen
GERMANY

Abstract: - Numerical simulations on impeller-diffuser interactions are performed in CFX-10 to investigate the unsteady phenomena, and the radial gap effects are also studied by calculating two different impeller-diffuser configurations. Computational results show that the leading edge of a diffuser vane acts as a source to the impeller unsteadiness. The diffuser-induced pressure fluctuation in the impeller increases with increasing radius, and the one on the impeller pressure side is much bigger than on the suction side. When increasing the radial gap between the impeller and the diffuser from 3% to 10% of the impeller outlet radius, the pressure fluctuation in the impeller decreases significantly. However, it has no evident influence on the time-averaged pressure field in the impeller.

Key-Words: - Impeller-diffuser interactions, numerical simulation, pressure fluctuation, radial gap

1 Introduction

The flow in a vaned diffuser radial pump is characterized by strongly unsteady interactions due to the relative motion and close proximity between the rotating impeller and the stationary diffuser, known as impeller-diffuser interactions, resulting in big pressure fluctuations both downstream and upstream. These fluctuations not only generate noise and vibrations, but also introduce unfavorable characteristics to pump performance even at the design point. Therefore, it is important to understand the sources of unsteadiness to control the pressure fluctuations and to improve the pump performance and reliability.

Some research work was conducted for a better understanding of pressure fluctuations related to impeller-diffuser interactions in radial pumps. Qin and Tsukamoto [1] calculated pressure fluctuations in the diffuser region through a two-dimensional singularity method. Wang and Tsukamoto [2, 3] developed a two-dimensional vortex method to investigate pressure fluctuations in the diffuser region. Shi and Tsukamoto [4] studied pressure fluctuations in the diffuser region by a CFD code STAR-CD. Furthermore, some experiments were performed to measure pressure fluctuations in diffuser radial pumps by Arndt et al. [5], Justen et al. [6], Furukawa et al. [7], Guo and Maruta [8].

The radial gap between the impeller outlet and the diffuser vane inlet has been reported to be an important factor to the unsteady phenomena. For example, Qin and Tsukamoto [9] studied the gap effect on pressure fluctuations in the diffuser region by a two-dimensional inviscid simulation. Arndt et al. [10] measured the pressure fluctuations in the diffuser region with two different radial gaps.

This work focuses on the radial gap effects on the diffuser-induced impeller flow, especially on the pressure fluctuation in the impeller region, in a radial pump stage consisting of an impeller, a vaned diffuser and a vaned return channel. Two different radial gaps between the impeller outlet and the diffuser vane inlet are calculated by the CFD code CFX-10. Numerical results for both cases are compared and discussed in detail.

2 Numerical analysis

The test pump stage consists of an impeller, a vaned diffuser and a vaned return channel. The impeller is shrouded with six strongly backswept blades. Two kinds of diffusers are equipped here with different vane inlet radii: 77.5 and 82.8 [mm], corresponding to the radial gap of 3% and 10% of the impeller outlet radius, respectively. Both the diffuser and the return channel have nine vanes. All blades and vanes are designed in two dimensions with constant thickness for the convenience of further PIV measurements. The specifications of the pump stage are illustrated in Table 1.

Table 1 Specifications of the pump stage

Number of impeller blades	Z_i	6
Impeller inlet radius	R_1	40 mm
Impeller outlet radius	R_2	75.25mm
Number of diffuser vanes	Z_d	9
Diffuser inlet radius	R_3	77.5 mm
		82.8 mm
Diffuser outlet radius	R_4	95 mm
Number of return channel vanes	Z_r	9
Design flow rate	Q_{des}	$0.0045 m^3/s$
Design rotating speed	n_{des}	1450 rpm

The structured grid for the computational domains is created by using the grid generation tool ICEM-CFD, and the first grid node from the wall is well controlled to make y+ below 60 in the whole computational domains, enabling better boundary layer resolutions by wall functions. The grid at the midspan of the impeller and the diffuser is shown in Fig.1.

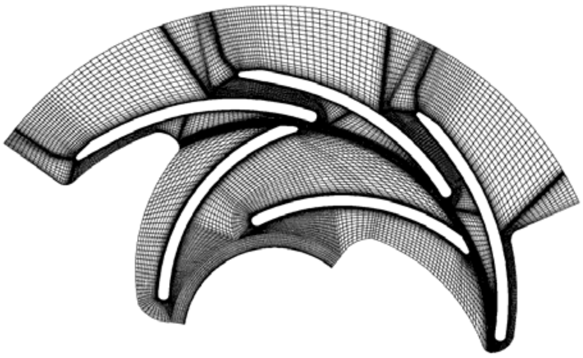

Fig.1 Grid view at midspan, 3% gap.

Only one third of the pump stage is simulated with periodic conditions because the blade number ratio is 6 (impeller): 9 (diffuser): 9 (return channel), which can be simplified to 2:3:3 under the guarantee of pitch ratio of unity. In this case, the total number of nodes is about 1.7 million. The expected periodicity of the flow field has been validated in our previous work [11].

In this work, three-dimensional, unsteady Reynolds-averaged Navier-Stokes equations are solved by the CFD code CFX-10, in which a finite volume method is utilized. For boundary conditions, the total pressure and the absolute velocity direction are imposed at the inlet, and the mass flow is given at the outlet. A no-slip wall condition is given for the flow at the wall boundaries of the hubs, the shrouds, the blades and the vanes. The turbulence is simulated by the shear stress transport (SST) turbulence model with automatic near wall treatments [12], with 5% intensity and a viscosity ratio of 10. The discretization in space is of second order accuracy. The second order backward Euler scheme is chosen for the time dependent terms. The interface between the impeller and the diffuser is set to “transient rotor-stator”, in which the relative position between the rotor and the stator is updated each time step. The time step is set to 1.14942×10^{-4} [s], corresponding to a rotating angle change of $\Delta\varphi = 1$ [deg] per time step in the case of the rotating speed of 1450 [rpm]. The maximum number of iterations for each time step is set to 10 in order to reduce all maximum residuals below 10^{-3}. Before the transient simulation, a steady simulation is performed with the interface of “frozen rotor”, and the steady result is used as an initial guess. The rotating angle φ defined in Fig. 2 is used to indicate the relative position between the impeller and the diffuser. Some monitor points are placed in the computational domains, one of which marked in crosshair is at the impeller trailing edge, used to judge the periodic convergence of the unsteady flow calculation.

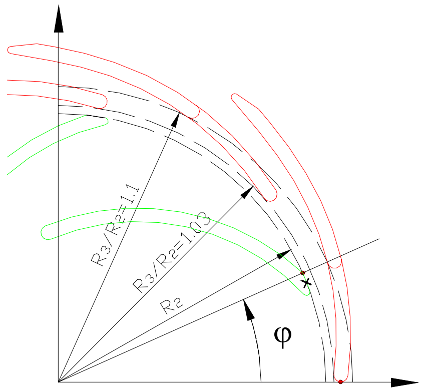

Fig.2 Schematics of the pump and the definition of rotating angle.

3 Results

All results discussed in this paper are limited to the design operating point of the pump A periodic flow field is achieved after 20 impeller revolutions judged by the pressure at the monitor points. After that, one more impeller revolution is calculated further to get transient statistics of the results, in which the maxima, the minima and the time averages of the pressure and the velocity on each grid node in the computational domains are recorded. Afterwards, the peak-to-peak difference of pressure fluctuation, normalized by the dynamic pressure based on the impeller tip speed U_2, on a grid node is calculated by Eq. (1); the normalized standard deviation of pressure fluctuation is also defined in Eq. (2),

Proceedings of the 4th WSEAS International Conference on Fluid Mechanics and Aerodynamics, Elounda, Greece, August 21-23, 2006 (pp289-294)

$$(C_P)_{p-p} = \frac{\Delta p}{\frac{1}{2}\rho U_2^2} = \frac{(p_{\max} - p_{\min})}{\frac{1}{2}\rho U_2^2} \qquad (1)$$

$$(C_p)_{sdv} = \frac{\sqrt{\frac{1}{N}\sum_{j=1}^{N}(P_j - \overline{P})^2}}{\frac{1}{2}\rho U_2^2} \qquad (2)$$

where, $p_{\max}$, $p_{\min}$ and $\overline{p}$ are the maximum, the minimum and the time-averaged pressure on the grid node during one impeller revolution. N is the sample number during one period, i.e. the number of time steps in one period.

The stator-induced unsteady secondary relative velocity vector at one time instant is illustrated in Fig.3. These vectors show only the periodic components of the velocity by subtracting the time-averaged one, which represent the part of the flow changing periodically with the blade passing frequency. Note that a vector pointing in the reverse direction of the flow does not indicate reverse flow but only denotes that the current velocity level is smaller than the average value. A local high periodic velocity region is located just opposite to a diffuser vane leading edge. It is obvious that the leading edge of a diffuser vane acts as a source to the impeller-diffuser interactions.

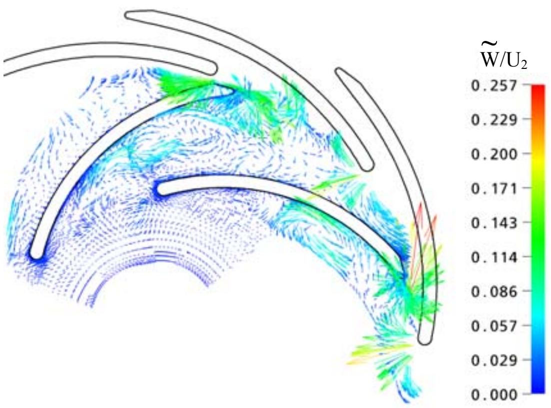

Fig.3 Unsteady secondary relative velocity vector ($W - \overline{W}$) at midspan of the impeller, 3% gap.

The standard deviation of pressure fluctuation at midspan of the impeller is plotted in Fig.4. The strong pressure fluctuations at the impeller outlet, due to the unsteady interactions between the impeller blades and the diffuser vanes, are also reflected upstream to the impeller inlet [13]. In general, the fluctuation decreases with increasing radius, and the biggest one occurs at the impeller outlet, reaching 0.085. Note that there is a small region in the middle chord of the impeller pressure side where the pressure fluctuation decreases slightly when the radius increases. It is also found that the pressure fluctuation on the pressure side of the impeller is much bigger than on the suction side for a given radius. This trend is becoming more evident at the rear part of the impeller blade. The reason may be that the diffuser vane leading edge can not impinge directly on the impeller suction surface, i.e. the impeller pressure side is more exposed to the potential interactions between the impeller and the diffuser compared to the impeller suction side.

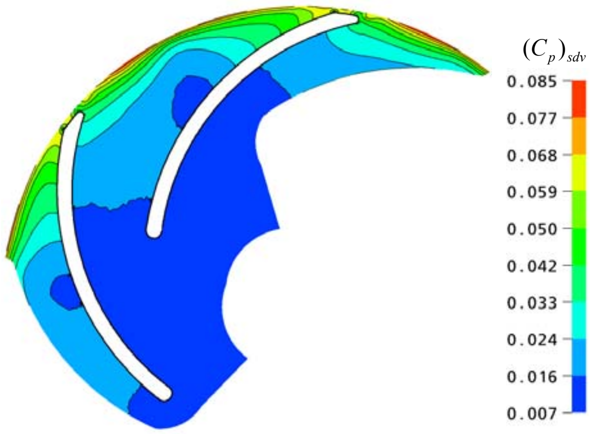

Fig.4 Pressure fluctuation at midspan of the impeller, 3% gap.

As defined above, there are two means to determine the pressure fluctuation: the standard deviation and the peak-to-peak difference of pressure. The pressure fluctuations obtained by the two methods are compared at the midspan of the impeller blade in Fig.5. It seems that two methods predict nearly the same trend on pressure fluctuation. Therefore, the standard deviation of pressure fluctuation is in accordance with the peak-to-peak one.

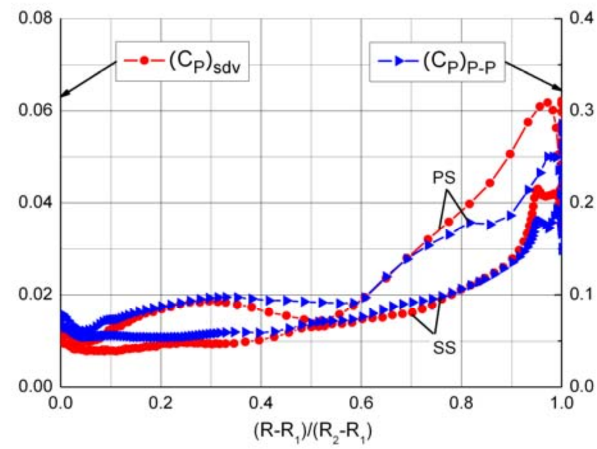

Fig.5 Pressure fluctuation comparison between standard deviation and peak-to-peak difference.

In the following part, the gap effects on the impeller transient phenomena are analysed by comparing the results obtained by calculations for two different radial gaps between the impeller outlet and the diffuser vane inlet: 3% and 10% of the impeller outlet radius, respectively.

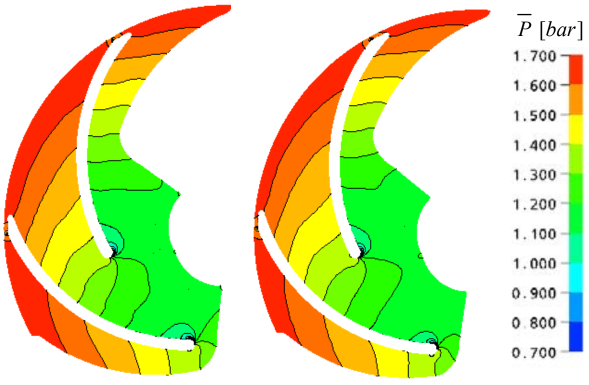

(a) 3% gap (b)10% gap

Fig.6 Time-averaged pressure field at midspan of the impeller.

The time-averaged pressure fields at the impeller midspan are compared in Fig.6. For both gaps, the pressure fields are quite similar, and nearly no difference can be observed: the pressure increases gradually and uniformly from the impeller inlet to the outlet, and the pressure on the impeller pressure side is bigger than on the suction side. Therefore, the change of radial gap between the impeller and the diffuser has no evident effect on the time-averaged impeller pressure field.

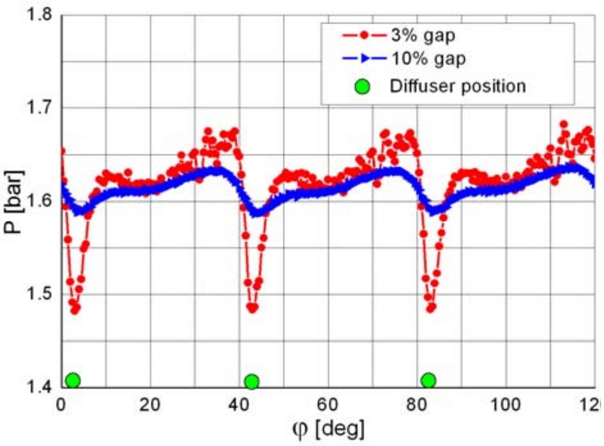

Fig.7 Pressures at the monitor point at the impeller trailing edge.

The comparison of pressure history in one period at the monitor point (in the middle of the impeller trailing edge) versus the rotating angle for two radial gaps is given in Fig. 7, and the position of diffuser vanes are marked at the bottom of the figure for clarity. For both cases, the pressure reaches a local minimum when the monitor point is just positioned opposite to the diffuser vane leading edge. When a diffuser channel is fully overlapped by an impeller channel, the pressure reaches a peak. Concerning the gap effect, the pressure valley for the 3% gap is much smaller than that for 10% gap. Thus, the diffuser effect on the pressure fluctuation is much bigger for 3% gap than for 10% gap.

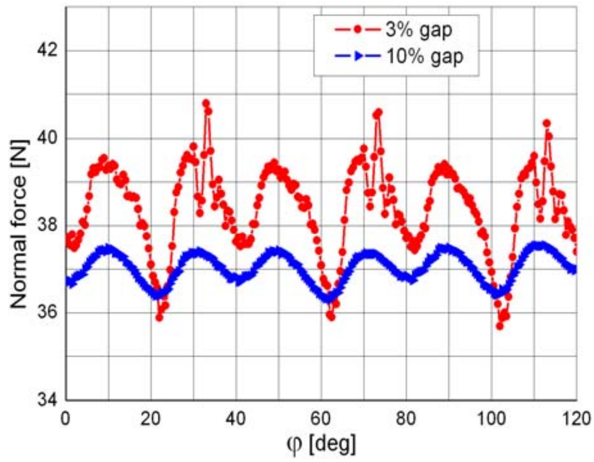

Fig.8 Comparison of total normal force on the impeller blade surfaces.

The comparison of total normal force on the two simulated impeller blades between two radial gaps caused by the unsteady pressures is plotted in Fig.8, with the function of the rotating angle. For both cases, the force exhibits a good periodicity for each diffuser vane circumferential pitch. When the suction side of an impeller trailing edge approaches a diffuser vane leading edge ($\varphi=4^0$, 24^0, 44^0, 64^0, 84^0, 104^0), the total normal force for both radial gaps attains a local minimum. When a diffuser vane leading edge is located in the middle of an impeller flow passage ($\varphi=10^0$, 50^0, 90^0), i.e. the impeller passage is bisected by the diffuser, and when a diffuser channel is fully overlapped by an impeller channel ($\varphi=30^0$, 70^0, 110^0), the total normal force on two impeller blades reaches a local maximum. For 3% gap, the force changes dramatically after the overlapping process: it decreases rapidly and increases back to a peak within a rotating angle change of 3 [deg]. However, this phenomenon can not be observed in the case of 10% gap. It is also found that both the average value and the fluctuation amplitude of the total normal force decrease greatly when the radial gap increases from 3% to 10%.

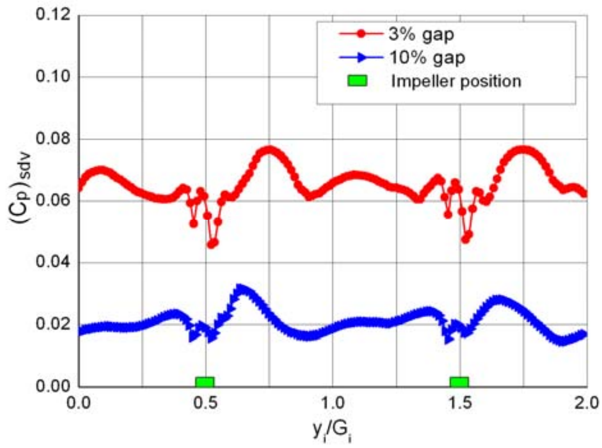

Fig.9 Comparison of pressure fluctuation at the impeller outlet (R/R_2=1.01) at midspan.

The normalized pressure fluctuation at the impeller outlet is plotted at midspan in Fig.9, with the impeller positions indicated at the bottom of the figure. For both cases, a similar pressure fluctuation distribution trend can be observed, and the highest one occurs in the blade passage. There is an obvious change in fluctuation amplitude in the region where the impeller trailing edge is faced. Furthermore, when the radial gap increases from 3% to 10%, the amplitude of the pressure fluctuation is decreasing from the level of 0.6 to 0.2, accounting for about 60% in relative reduction.

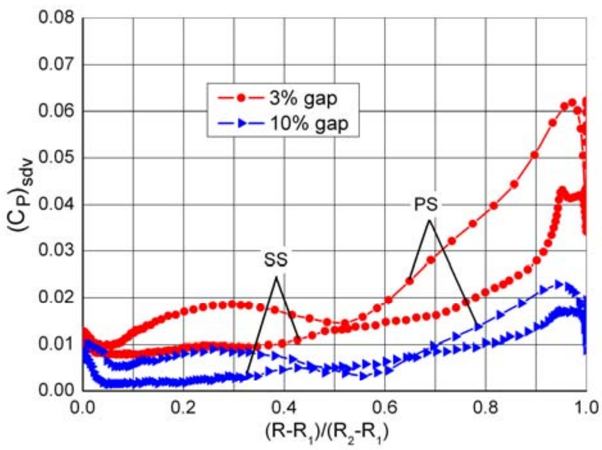

Fig.10 Comparison of pressure fluctuation on the impeller blade surface at midspan.

The normalized pressure fluctuations on the impeller blade surface are plotted for both gaps at midspan in Fig. 10. The biggest one is found at the impeller trailing edge. For both cases, the pressure fluctuation on the suction side (SS) keeps increasing with the increase of radius. However, the one on the pressure side (PS) is decreasing in the range of relative radius between 0.3 and 0.5. The increase in pressure fluctuation becomes bigger at the impeller rear part. For 3% gap, the pressure fluctuation on the pressure side is bigger than that on the suction side for the whole range, which has been found experimentally by Arndt et al. [5, 10]. However, for the case of 10% gap, there is a small region in the middle chord where the fluctuation on the pressure side is smaller than on the suction side. As for radial gap effect on the pressure fluctuation, it is rather evident that increasing radial gap results in a reduction of around 60% in the amplitude of pressure fluctuation on the impeller blade surface, and this trend is more evident in the rear part of the impeller blade. In addition, the gap influence on the pressure fluctuation is bigger on the impeller blade pressure side than on the suction side.

4 Conclusions

Numerical simulations are performed to investigate the impeller-diffuser interactions in a diffuser pump in CFX-10, and the radial gap effects are also studied. It is found that:

- The leading edge of a diffuser vane acts as a source to the impeller unsteadiness.
- The biggest pressure fluctuation on the impeller blade surface is found at the trailing edge.
- The pressure fluctuation on the impeller suction side keeps increasing with the increase of radius. However, there is a small region on the pressure side where the fluctuation decreases slightly with increasing radius.
- The change of the radial gap has no obvious evident effect on the time-averaged impeller pressure field.
- Increasing the radial gap from 3% to 10 % (based on the impeller outlet radius) reduces significantly the pressure fluctuation by about 60% on impeller blade surface. Consequently, both the average value and the fluctuation amplitude of the total normal force on the impeller blades decrease greatly.
- The gap influence on the pressure fluctuation is bigger on the impeller blade pressure side than on the suction side.

Nomenclature

C_P	pressure coefficient
f	frequency
G	circumferential pitch
n	rotating speed
P	static pressure
PS	pressure side

Q	volume flow rate
R	radius
SS	suction side
W	relative velocity
y	circumferential coordinate
Z	blade number
φ	rotating angle
ρ	density of water
ω	rotating speed

Subscripts

1	impeller inlet
2	impeller outlet
3	diffuser inlet
4	diffuser outlet
d	diffuser
des	design operating point
i	impeller
p-p	peak to peak difference
sdv	standard deviation

Superscripts

—	time-averaged in one period
~	periodic component

References:

[1] Qin, W. and Tsukamoto, H., Theoretical Study of Pressure Fluctuations Downstream of a Diffuser Pump Impeller-Part 1: Fundamental Analysis on Rotor-Stator Interaction, *Journal of Fluids Engineering*, Vol.119, 1997, pp. 647-652.

[2] Wang, H. and Tsukamoto, H., Fundamental Analysis on Rotor-Stator Interaction in a Diffuser Pump by Vortex Method, *Journal of Fluids Engineering*, Vol.123, 2001, pp. 737-747.

[3] Wang, H., and Tsukamoto, H., Experimental and Numerical Study of Unsteady Flow in a Diffuser Pump at Off-Design Conditions, *Journal of Fluids Engineering*, Vol.125, 2003, pp.767-777.

[4] Shi, F. and Tsukamoto, H., Numerical Study of Pressure Fluctuations Caused by Impeller-Diffuser Interaction in a Diffuser Pump Stage, *Journal of Fluids Engineering*, Vol.123 , 2001, pp.466-474.

[5] Arndt, N., Acosta, A.J., Brennen, C.E., and Caughey, T.K., Experimental Investigation of Rotor-Stator Interaction in a Centrifugal Pump with Several Vaned Diffusers, *Journal of Turbomachinery*, Vol.112, 1990, pp. 98-108.

[6] Furukawa, A., Takahara, H., Nakagawa, T., and Ono, Y., Pressure Fluctuation in a Vaned Diffuser Downstream from a Centrifugal Pump Impeller, *International Journal of Rotating Machinery*, Vol. 9, 2003, pp.285–292.

[7] Justen, F., Ziegler, K.U., and Gallus, H.E., Experimental Investigation of Unsteady Flow Phenomena in a Centrifugal Compressor Vaned Diffuser of Variable Geometry, Proceedings of 43rd International Gas Turbine and Aeroengine Congress and Exhibition, Stockholm, Sweden, June 2-5 1998.

[8] Guo, S., and Maruta, Y., Experimental Investigations on Pressure Fluctuations and Vibration of the Impeller in a Centrifugal Pump with Vaned Diffuser, *JSME International Journal, Series B: Fluids & Thermal Engineering*, Vol.48, 2005, pp.136-143.

[9] Qin, W., and Tsukamoto, H., Theoretical Study of Pressure Fluctuations Downstream of a Diffuser Pump Impeller-Part 2: Effects of volute, flow rate and radial gap, *Journal of Fluids Engineering*, Vol.119, 1997, pp. 653-658.

[10] Arndt, N., Acosta, A.J., Brennen, C.E., and Caughey, T.K., Rotor-Stator Interaction in a Diffuser Pump, *Journal of Turbomachinery*, Vol.111, 1989, pp. 213–221.

[11] Benra, F.-K., Feng, J., Dohmen, H.J., Numerical Study on Pressure Fluctuations in a Complete Stage of a Centrifugal Pump, The Eleventh International Symposium on Transport Phenomena and Dynamics of Rotating Machinery, Hawaii, USA, Feb.26-Mar. 2, 2006.

[12] Menter, F. R., Two-equation Eddy-viscosity Turbulence Models for Engineering Applications, AIAA-Journal, Vol.32, 1994, pp. 1598-1605.

[13] Dring, R.P., Joslyn, H.D., Hardwin, L.W., and Wagner, J.H., Turbine rotor-stator interaction, ASME Journal of Engineering Power, Vol.104, 1982, pp.729-742.